Do Radio Core-Halos and Cold Fronts in Non-Major-Merging Clusters Originate from the Same Gas Sloshing?

2008 ApJ 675 L9

(http://iopscience.iop.org/1538-4357/675/1/L9)

The Astrophysical Journal, 675: L9–L12, 2008 March 1

DO RADIO CORE-HALOS AND COLD FRONTS IN NON-MAJOR-MERGING CLUSTERS ORIGINATE FROM THE SAME GAS SLOSHING?

Pasquale Mazzotta[1,2] and Simona Giacintucci[2,3]

Received 2007 December 5; accepted 2008 January 11; published 2008 January 28

ABSTRACT

We show an interesting correlation between the surface brightness and temperature structure of the relaxed clusters RX J1720.1+2638 and MS 1455.0+2232, hosting a pair of cold fronts, and their central core-halo radio source. We discuss the possibility that the origin of this diffuse radio emission may be strictly connected with the gas sloshing mechanism suggested to explain the formation of cold fronts in non-major-merging clusters. We show that the radiative lifetime of the relativistic electrons is much shorter than the timescale on which they can be transported from the central galaxy up to the radius of the outermost cold front. This strongly indicates that the observed diffuse radio emission is likely produced by electrons reaccelerated via some kind of turbulence generated within the cluster volume limited by the cold fronts during the gas sloshing.

Subject headings: cooling flows — galaxies: clusters: general — galaxies: clusters: individual (RX J1720.1+2638, MS 1455.0+2232) — X-rays: galaxies

Online material: color figures

1. INTRODUCTION

A number of cool-core clusters of galaxies host very peculiar diffuse radio sources at their center characterized by a *core-halo* (CH) structure (e.g., PKS 0745−191; Baum & O'Dea 1991). These objects show an amorphous steep-spectrum halo which surrounds a bright core coincident with the dominant galaxy, with no jets on the kiloparsec scale. Even though the connection between CHs and cool-core clusters is well established, the origin of these sources remains uncertain. Sarazin et al. (1995) argued that they might be produced by the interaction between the radio source and the thermal gas cooling at the cluster center, i.e., in the form of disruption of the jets by the high-pressure ambient medium and buoyant effects on the radio plasma from the disrupted jets. In this Letter we show an interesting spatial correlation between the CH emission and X-ray features in two galaxy clusters RX J1720.1+2638 ($z = 0.159$) and MS 1455.0+2232 ($z = 0.258$), both showing a pair of cold fronts (CFs) in their core. We suggest a connection between the origin of the CH structure and the same gas sloshing mechanism responsible for the formation of the CFs. We use $H_0 = 70$ km s^{-1} kpc^{-1}, $\Omega = 0.27$, and $\Lambda = 0.73$.

2. X-RAY DATA PREPARATION AND ANALYSIS

For the purpose of this Letter we provide a short summary of the X-ray data preparation and analysis. We refer to two companion papers for details (P. Mazzotta et al., in preparation). The analysis of RX J1720.1+2638 was performed combining three *Chandra* observations (OBS_ID = 1453, 3224, and 4631). A single *Chandra* observation (OBS_ID = 4192) was used for MS 1455.0+2232. After flare cleaning, the useful exposure time is 42,508 and 88,556 s for RX J1720.1+2638 and MS 1455.0+2232, respectively. All images are background subtracted and vignetting corrected. The spectral analysis was carried out in the 0.7–9 keV energy band in PI channels. The spectral fitting was performed assuming fixed absorption and metallicity appropriate for each cluster ($N_{\rm H} = 3.6 \times 10^{20}$ cm^{-2}, $Z = 0.39\ Z_\odot$ and $N_{\rm H} = 3.0 \times 10^{20}$ cm^{-2}, $Z = 0.5\ Z_\odot$ for RX J1720.1+2638 and MS 1455.0+2232, respectively). The temperature maps were produced using a radially increasing Gaussian smoothing of $\sigma = 1$ pixel in the center up to $\sigma = 10$ pixels in the more external regions (see Vikhlinin et al. 2001 for details).

3. X-RAY IMAGE AND TEMPERATURE MAP

Both RX J1720.1+2638 and MS 1455.0+2232 were known to host two sharp variations of the surface brightness (edges) on opposite sides with respect to the cluster center (Mazzotta et al. 2001a, 2001b). It was suggested that such features were CFs but no final conclusion was possible due to the limited statistics available. The new, deeper observations allow us to disentangle the nature of the observed edges. To better highlight the spatial structure of the edges, we created a ratio image for both clusters by dividing the photon image in the [0.5, 2.5] keV energy band by its radial mean values simply obtained from the radial profile centered in the X-ray peak. The resulting image was smoothed using a top-hat function with $r = 3$ pixels. The ratio image and projected temperature map of RX J1720.1+2638 are shown in the left and right panels of Figure 1, respectively. Overlaid are the 1.5 GHz radio contours (from VLA-B archive data) of the central CH. In the left and right panels of Figure 2 we show the same images for MS 1455.0+2232, overlaid with the Giant Metrewave Radio Telescope (GMRT) 610 MHz contours. Figures 1 and 2 clearly show that the edges appear as part of a more extended spiral-like excess structure at the center of both clusters. They seem to confine the CH radio emission. Furthermore, the radio structure appears spatially correlated with the X-ray excess, following the spiral pattern in its more external regions.

4. COLD FRONTS

In this section we demonstrate that all the edges indicated by black lines in Figures 1 and 2 are CFs. We provide a brief description of these features, and refer to the forthcoming papers for a detailed analysis and discussion. For each edge we

[1] Dipartimento di Fisica, Universitá di Roma "Tor Vergata," Via della Ricerca Scientifica 1, I-00133 Rome, Italy; mazzotta@roma2.infn.it.

[2] Harvard-Smithsonian Center for Astrophysics, 60 Garden Street, Cambridge, MA 02138.

[3] INAF–Istituto di Radioastronomia, via Gobetti 101, I-40129 Bologna, Italy; sgiaci_s@ira.inaf.it.

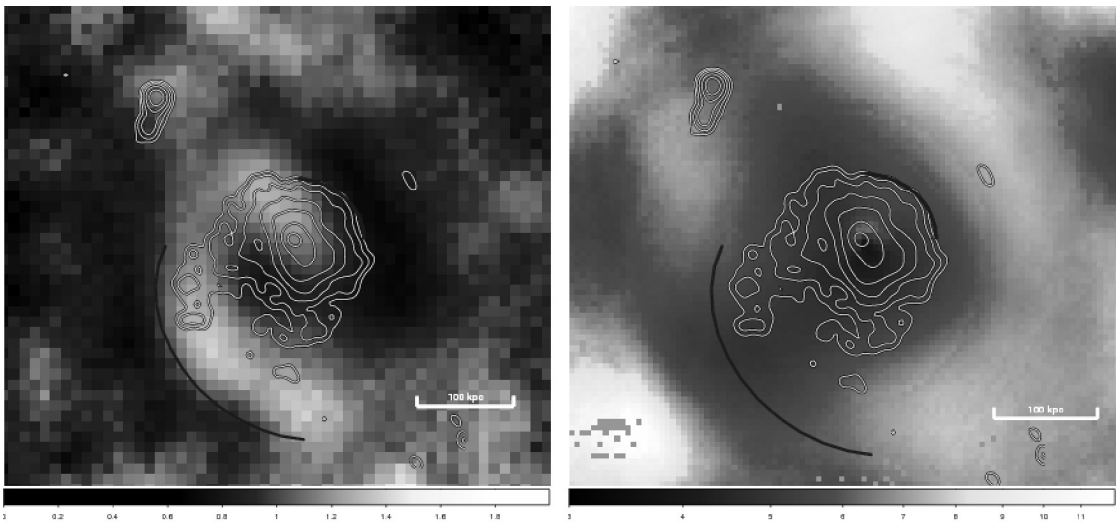

FIG. 1.—*Left*: Ratio *Chandra* X-ray image of RX J1720.1+2638 in the [0.5, 2.5] keV band overlaid on the 1.5 GHz VLA-B contours. The X-ray ratio image is obtained by dividing the actual cluster image by its radial mean values and by smoothing the result using a top-hat function with $r = 3$ pixels. Each pixel corresponds to 4″. Black lines indicate the position of the CFs. Radio contours are logarithmically spaced by a factor of 2 from 0.10 mJy beam^{-1}. The radio beam is 5.7″ × 4.8″. *Right*: X-ray projected temperature map of RX J1720.1+2638 in keV. Contours and lines as in the left panel. [*See the electronic edition of the Journal for a color version of this figure.*]

extracted the surface brightness profile within the relative sector. The centers and position angles for each sector are reported in Table 1. In Figures 3 and 4 we show the surface brightness and projected temperature profiles of the two sectors of RX J1720.1+2638 and MS 1455.0+2232, respectively. We modeled the edge using a simple analytic function for the electron density (n_e) and 3D temperature (T), both with a discontinuity (a jump) at the front:

$$n_e = n_0 \times \begin{cases} D_n (r/r_{\rm jump})^{\alpha_1}, & r < r_{\rm jump}, \\ (r/r_{\rm jump})^{\alpha_2}, & r > r_{\rm jump}, \end{cases} \quad (1)$$

and

$$T = T_0 \times \begin{cases} 1, & r < r_{\rm jump}, \\ D_T \left[\dfrac{1 + (r_{\rm jump}/r_T)^2}{1 + (r/r_T)^2} \right]^c, & r > r_{\rm jump}. \end{cases} \quad (2)$$

Assuming spherical symmetry we projected both density and temperature models, and fitted them simultaneously to the observed surface brightness and temperature profiles. For the temperature projection we used the spectroscopic like definition $T_{\rm sl}$ introduced by Mazzotta et al. (2004).

In Figures 5 and 6 we show the best fit within the 68% confidence level error curves relative to the density, temper-

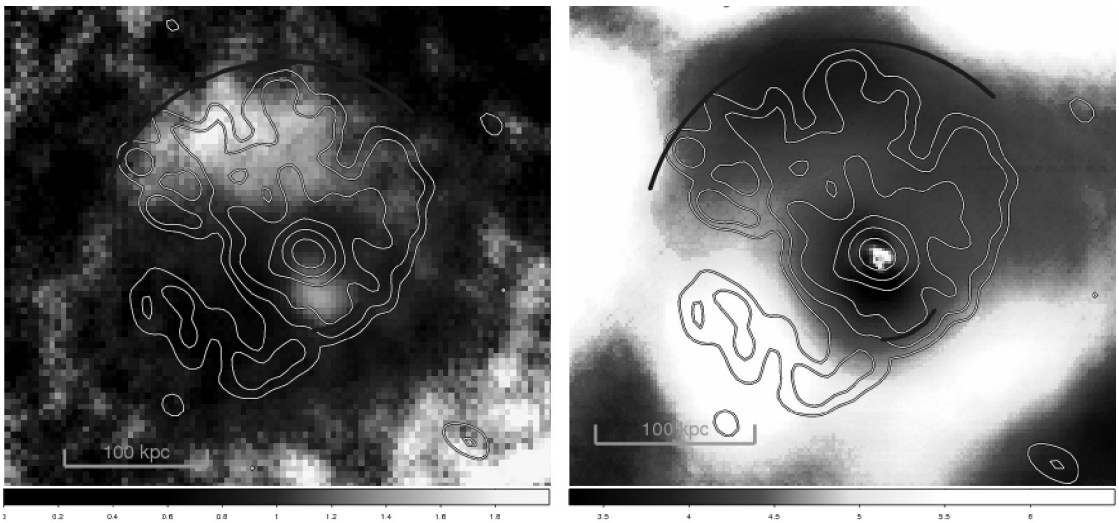

FIG. 2.—*Left*: Ratio *Chandra* X-ray image of MS 1455.0+2232 in the [0.5, 2.5] keV band overlaid on the GMRT 610 MHz contours. The X-ray ratio image is obtained by dividing the actual cluster image by its radial mean values and by smoothing the result using a top-hat function with $r = 3$ pixels. Each pixel corresponds to 1″. Black lines indicate the position of the CFs. Radio contours are logarithmically spaced by a factor of 2 from 0.15 mJy beam^{-1}. The radio beam is 5.9″ × 4.6″. *Right*: X-ray projected temperature map of MS 1455.0+2232 in keV. Contours and lines as in the left panel. [*See the electronic edition of the Journal for a color version of this figure.*]

TABLE 1
PARAMETERS OF THE COLD FRONTS

Sector	(x, y) (J2000.0)	Position Angle[a] (deg)	$r_{\rm jump}$ (Mpc)	D_n	D_T	r_T (Mpc)	c
RX J1720.1+2638:							
N	(17 20 10, +26 37 25)	2–80	0.0994 ± 0.0005	1.68 ± 0.03	1.68 ± 0.12	0.1	0
S	(17 20 10, +26 37 25)	180–280	0.1551 ± 0.0007	1.66 ± 0.05	1.49 ± 0.16	0.1	0
MS 1455.0+2232:							
N	(14 57 15, +22 20 35)	46–163	0.1367 ± 0.002	1.67 ± 0.06	1.72 ± 0.24	1.9 ± 0.3	2.6 ± 0.27
S	(14 57 15, +22 20 30)	270–330	0.0397 ± 0.003	1.50 ± 0.08	2.50 ± 0.30	0.23 ± 0.04	0.5 ± 0.10

[a] Position angles are measured anticlockwise from west.

ature, and pressure profiles of each edge. We also report as solid line the best-fit models of the surface brightness and temperature profiles to highlight the good agreement between the fit and the data. Furthermore, the middle panels of the same figures show the departures in sigmas of the surface brightness data with respect to the best fit. All the observed edges are CFs. We note that the pressure profile is continuous, within the errors, across the front (Table 1), so the speed of the fronts is highly subsonic.

5. DISCUSSION AND CONCLUSIONS

Using high-resolution simulations different authors showed that CFs in the core of relaxed galaxy clusters may be the result of gas sloshing induced by a minor merger with a small dark matter halo that occurred within the last few Gyr (see, e.g., Ascasibar & Markevitch 2006 [hereafter AM06] and references therein). The only condition for the CF to form is that the cluster have a steep entropy profile (as observed in cool core clusters) and the dark matter subhalo have a nonzero impact parameter. When the subhalo flies through the main cluster, it produces a gravitational disturbance that pushes the cool gas away from its initial position. This makes the gas slosh and two or more CFs form on opposite sides with respect to the cluster center. AM06 noticed that, when the gas is displaced from the center for the first time, it does not fall back radially, and the subsequent CF(s) is (are) not exactly concentric but combines into a spiral pattern (see 1.9–2.1 Gyr panels in Fig. 7 of AM06). As shown in § 3, both the CF pairs in RX J1720.1+2638 and MS 1455.0+2232, which are clearly two distinct nonconcentric structures, seem to combine into a spiral pattern very similarly to what is predicted by AM06. These structures are remarkably similar to the simulated ones in the surface brightness map (compare left panels of Figs. 1 and 2 with top left panel of Fig. 19 of AM06) as well as in the temperature map (compare right panels of Figs. 1 and 2 with bottom left panel of Fig. 19 of AM06). Thus the X-ray observations of these two clusters seem to confirm the prediction of AM06 for the gas sloshing.

What appears to be very interesting is that both clusters host a CH radio source. These sources seem to be well confined (in projection) within the CF pairs of the respective cluster. Furthermore, we noticed a spatial correlation between the radio emission and the X-ray spiral structure which might suggest that the radio-emitting electrons are trapped into the same ICM flows that produced the CFs. Given the lack of jets on the kiloparsec scale, the relativistic electrons need to be transported by some other mechanism from the central galaxy up to the radii of the outermost CFs. We might speculate that the relativistic electrons injected by the central AGN, and trapped into the ICM magnetic field, are transported at the CFs' radii by the motion of the low-entropy thermal gas induced by the gas sloshing. In fact, the AM06 simulations show that the CFs are formed by the continuous circulation of lower entropy gas that

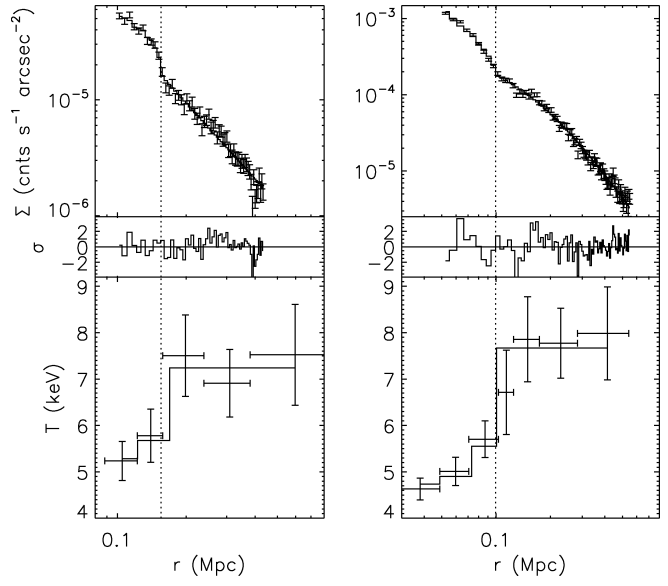

FIG. 3.—Projected surface brightness and temperature profiles of the cluster sectors containing the southeast (*left*) and northwest (*right*) CFs of RX J1720.1+2638. Vertical dotted lines indicate the positions of the edges. *Top panels*: Surface brightness profiles. The solid histograms are the projected best-fit models shown in the top panels of Fig. 5. *Middle panels*: Residuals of the surface brightness profile with respect to the best-fit model in sigmas. *Bottom panels*: Projected temperature profiles. The solid histograms are the projected best-fit models shown in the middle panels of Fig. 5.

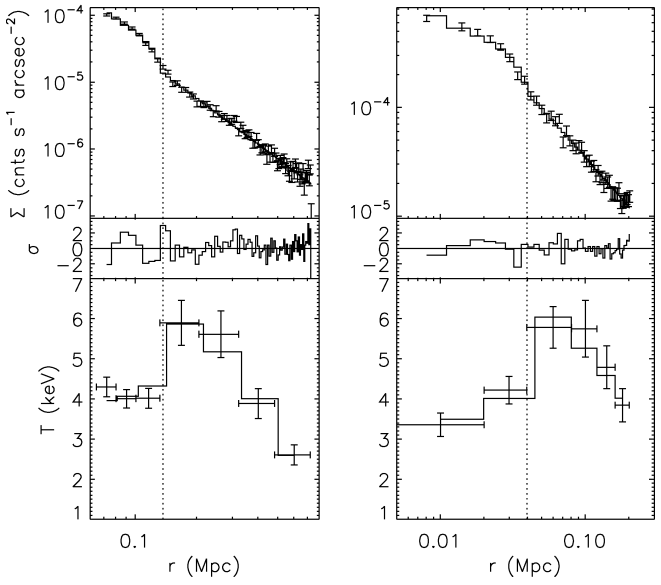

FIG. 4.—Same as in Fig. 3, but for the northeast (*left*) and southwest (*right*) CFs of MS 1455.0+2232.

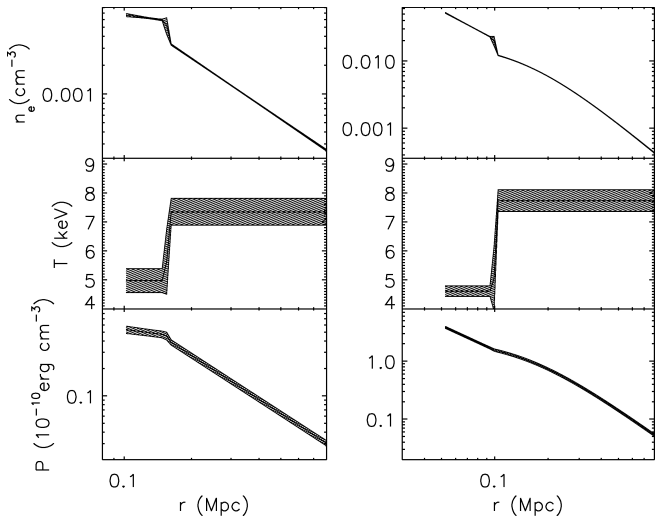

FIG. 5.—Electron density (n_e), temperature (T), and thermal pressure (P) profiles of the sectors containing the southeast (*left*) and northwest (*right*) CFs of RX J1720.1+2638. The shaded regions indicate the relative 68% confidence level errors.

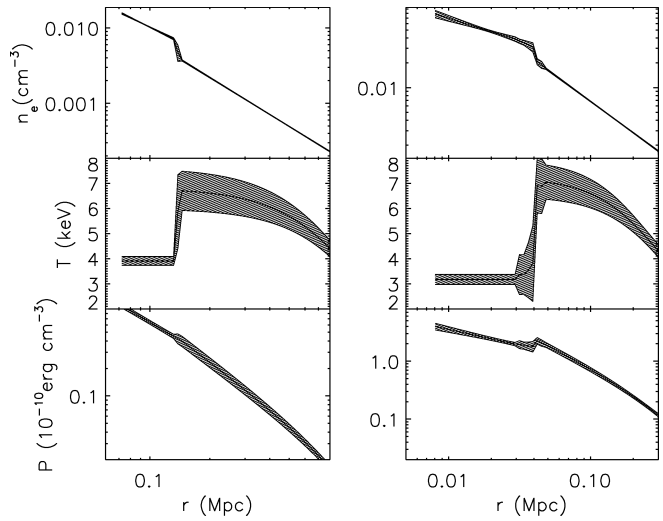

FIG. 6.—Same as in Fig. 5, but for the northeast (*left*) and southwest (*right*) CFs of MS 1455.0+2232.

comes from the inner core region and falls back soon after (see Fig. 7 of AM06). However, AM06 show that the speed of this gas circulation is relatively low with an upper limit of $v_{\max} = 500$ km s^{-1}. In both clusters the outermost CF is at a radial distance of $\Delta r \approx 150$ kpc. Assuming radial transport, we estimate that the minimum time needed for the relativistic electrons to be displaced up to the position of the outermost front is $t_{\min} \gtrsim 3 \times 10^8$ yr. This time is much larger than the radiative lifetime of relativistic electrons which suffer energy losses mainly due to inverse Compton scattering with the cosmic microwave background photons [$t \approx (10^7$–$10^8)/(1 + z)^4$ yr; see, e.g., Brunetti et al. 2001]. This simple calculation suggests that the observed radio emission might be produced by reacceleration of a population of relic electrons, injected into the ICM by a previous activity of the central AGN. Due to the subsonic nature of the gas sloshing, we can exclude that the reacceleration may be driven by thermal shock. An alternative and plausible mechanism may be reacceleration by MHD turbulence, as suggested to explain the cluster minihalos (Gitti et al. 2002) and giant radio halos (e.g., Brunetti et al. 2004). These authors claim that this reacceleration mechanism requires only a modest level (a few percent) of turbulence. In fact, 2D simulations with much higher resolutions have shown that the gas sloshing could automatically create turbulence in a core (e.g., Fujita et al. 2004).

It is worth noting that the CH/CFs correlation described in this Letter is not limited to these two clusters but seems to be present also in other clusters hosting a CH, such as, e.g., 2A 0335+096 (Mazzotta et al. 2003), PKS 0745−191 (Baum & O'Dea 1991), and A2052 (Zhao et al. 1993). These results call for further and deeper investigation of the radio–X-ray connection in relaxed clusters with CFs, which will be addressed in forthcoming papers.

We thank M. Markevitch, G. Brunetti, T. Venturi, and A. Vikhlinin for constructive criticism. This work was supported by contract ASI-INAF I/023/05/0, CXC grants AR6-7015X and GO5-6124X, NASA grant NNG04GK72G, and the Smithsonian Institution.

REFERENCES

Ascasibar, Y., & Markevitch, M. 2006, ApJ, 650, 102 (AM06)
Baum, S. A., & O'Dea, C. P. 1991, MNRAS, 250, 737
Brunetti, G., Blasi, P., Cassano, R., & Gabici, S. 2004, MNRAS, 350, 1174
Brunetti, G., Setti, G., Feretti, L., & Giovannini, G. 2001, MNRAS, 320, 365
Fujita, Y., Matsumoto, T., & Wada, K. 2004, ApJ, 612, L9
Gitti, M., Brunetti, G., & Setti, G. 2002, A&A, 386, 456
Mazzotta, P., Edge, A. C., & Markevitch, M. 2003, ApJ, 596, 190
Mazzotta, P., Markevitch, M., Forman, W. R., Jones, C., Vikhlinin, A., & VanSpeybroeck, L. 2001a, preprint (astro-ph/0108476)
Mazzotta, P., Markevitch, M., Vikhlinin, A., Forman, W. R., David, L. P., & VanSpeybroeck, L. 2001b, ApJ, 555, 205
Mazzotta, P., Rasia, E., Moscardini, L., & Tormen, G. 2004, MNRAS, 354, 10
Sarazin, C. L., Baum, S. A., & O'Dea, C. P. 1995, ApJ, 451, 125
Vikhlinin, A., Markevitch, M., & Murray, S. S. 2001, ApJ, 551, 160
Zhao, J.-H., Sumi, D. M., Burns, J. O., & Duric, N. 1993, ApJ, 416, 51